J. Phys. D: Appl. Phys. **44** (2011) 355203 (4pp) doi:10.1088/0022-3727/44/35/355203

Ion emission in collisions between two laser-produced plasmas

P Hough[1], P Hayden[1], C Fallon[1], T J Kelly[1], C McLoughin[1], P Yeates[1], J P Mosnier[1], E T Kennedy[1], S S Harilal[2] and J T Costello[1]

[1] School of Physical Sciences and National Centre for Plasma Science and Technology (NCPST), Dublin City University, Glasnevin, Dublin 9, Ireland
[2] School of Nuclear Engineering and Center for Materials under Extreme Environment, Purdue University, West Lafayette, IN 47907, USA

E-mail: padraighough@gmail.com and Patrick.Hayden@dcu.ie

Received 9 May 2011, in final form 19 July 2011
Published 16 August 2011
Online at stacks.iop.org/JPhysD/44/355203

Abstract
Measurements of the total ion emission from a pair of colliding laser-produced aluminium plasmas were obtained with the aid of a Faraday cup detector. The energy profile width at half height of the kinetic energy distribution for ions emitted normal to the target was found to be 30% narrower for colliding plasmas compared with a single plasma. Similar to ion emission from single plumes, the mean ion kinetic energy is observed to increase with the energy of the incident laser pulse. However, the width of the ion energy distribution increases at a significantly slower rate than in the single plume case.

(Some figures in this article are in colour only in the electronic version)

1. Introduction

Laser-produced plasmas (LPPs) are formed when the output pulse from a high power laser is focused onto a dense target at an irradiance typically in excess of $1\,\mathrm{GW\,cm^{-2}}$. LPPs have been the focus of strong fundamental research interest since their discovery in the 1960s [1] and have spawned a wide range of applications including laser induced breakdown spectroscopy, LIBS [2], pulsed laser deposition (PLD) [3], tabletop sources of short wavelength light [4], ion sources [5], high harmonic generation [6] and laboratory simulations of astrophysical plasmas [7–9].

When two plasmas collide, under appropriate conditions, as outlined by Rambo *et al* [10], a layer of stagnated plasma is formed at the collision front. Outside these conditions the colliding plasmas undergo interpenetration where the plasmas pass through each other without stagnating. Rambo *et al* introduced the so-called 'collisionality parameter,' ζ, to determine whether stagnation or interpenetration will dominate in colliding plasmas. The collisionality parameter is given by

$$\xi = \frac{L}{\lambda_{ii}},$$

where L is the typical plasma dimension (i.e. the separation between the two colliding plasmas) and λ_{ii} is the ion–ion mean free path given by [11]

$$\lambda_{ii} = \frac{m_i^2 \upsilon_{12}^2}{4\pi e^4 Z^4 n_i \ln \Lambda_{12}},$$

where m_i is the ion mass, ν_{12} is the relative collision velocity, e is the charge of the electron, Z is the average ionization state of the plasma, n_i is the average plasma ion density and $\ln \Lambda_{12}$ is the so-called Coulomb logarithm [12] for collisions between the individual plasma plumes.

Colliding LPPs were first investigated, to the best of the authors' knowledge, in the mid-1970s [13]. Significant work was carried out subsequently on high-energy colliding plasmas with laser intensities $\sim 10^{14}\,\mathrm{W\,cm^{-2}}$ [14], especially, but not exclusively on, indirect drive fusion [15]. In indirect fusion devices a hollow hohlraum hosts multiple colliding plasmas as x-ray sources which are used to drive fusion in a fuel cell located at the centre of the hohlraum [16]. Colliding plasmas have also shown much potential as laboratory scale models of astronomical interactions where, for example, Gregory *et al* [17] and Smith *et al* [18] have shown how they can be used as a scaled model of astrophysical colliding shocks. At lower

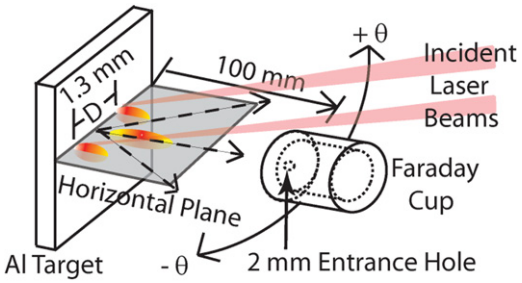

Figure 1. Schematic diagram of the experimental configuration (not to scale). The seed plasmas were separated by a distance of 1.3 mm, the Faraday cup was located at a distance of 100 mm from the target and the entrance aperture of the Faraday cup was 2 mm in diameter.

laser intensities, in the range of interest here, colliding plasmas show real promise for applications in thin film deposition. For example, recently droplet free films were successfully fabricated using colliding LPPs [19].

To date we have reported a number of time resolved spectroscopic and imaging studies on the evolution of low-energy laser-produced colliding plasmas [20–23]. In this paper we change our focus to the ion emission from the colliding plasma system. In particular, we extract the angularly resolved ion energy distributions. In fact, a lot of work has been carried out using ions from LPPs for ion bunch injection into accelerators for medical, industrial and research and development purposes [24, 25]. Areas such as ion implantation [26] and surface etching [24] have benefited significantly from the development of the laser ion source. Other potential applications of laser ion sources are varied and growing with significant effort being invested in areas such as cancer therapy [27]. Hence, the results reported here may be of interest to several apposite groups.

2. Experiment

The experimental scheme is illustrated in figure 1 showing how laterally colliding plasmas were used to generate the ions. A Nd : YAG laser beam of wavelength 1064 nm and a whole beam energy of 600 mJ, with a pulse width of 6 ns (full width at half maximum (FWHM)), was split into two equal parts and focused to two spots (i.e. 300 mJ at each focal point) separated by a distance of 1.3 mm on an aluminium slab target. The spotsize at each focus was $\sim$100 μm yielding an irradiance of 3×10^{11} W cm^{-2} and we refer to the pair of plasmas so formed as 'seed plasmas'. A Faraday cup, which could be rotated about the target normal in the horizontal plane (as illustrated in figure 1) with an accuracy of $\pm 1^{\circ}$, was placed so that it directly faced the target at a distance of 10 cm from the target. The entrance aperture was a 2 mm circular hole and a bias voltage of -30 V was applied to the cup to collect the ions. The signals were collected across a 50 Ω resistor coupled to a digital oscilloscope operated in single shot mode. All experiments were performed at a base pressure of 1×10^{-5} mbar. The target was mounted on an in-vacuum high precision x-z motorized stage and was moved to reveal a fresh surface after each laser pulse.

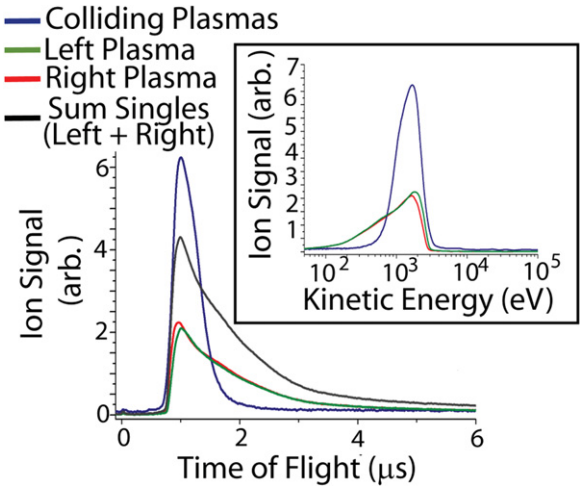

Figure 2. (Main) Ion TOF signals for colliding plasmas (dark blue trace) and single seed plasmas (red and green traces). The Faraday cup was positioned normal to the target. (Inset) TOF signals converted to kinetic energy distributions for single 'seed' plumes and colliding plasmas system.

3. Results and discussion

Ion emission was measured in both single and colliding plasma experiments. To generate the single laser plasma plumes, we simply blocked one of the split laser beams before it reached the target. Figure 2 (main) shows a comparison of the ion time of flight (TOF) signals collected for the colliding plasmas system (dark blue trace) along with those for the single seed plasma cases (red and green traces). The numerical sum of the left and right plasma distributions is also shown in the figure (black trace). The corresponding kinetic energy distributions derived from the TOF profiles are shown in figure 2 (inset).

In the case of colliding plasmas, a stagnation layer results from a rapid accumulation of seed plasma material at the collision front between the two plumes [21]. As shown in figure 2 (main), the TOF profile observed for the colliding plasmas was found to be noticeably narrower than that obtained from either of the individual seed plasmas which have almost identical profiles. In figure 2 (inset) the TOF scale is converted to kinetic energy and it reveals a redistribution of the translational energy of the ions emitted in the colliding plasma case into a narrower profile compared with the individual single seed plumes. The low energy tail present in the kinetic energy distribution for the single plasma case is significantly attenuated in the colliding plasma case, resulting in a narrower and more symmetric distribution. Typically, the ions emitted from a single laser-produced plasma, possess an asymmetric distribution [28]. The distribution for the seed plasmas here ranges from $\sim$0.1 to 3 keV with a width (at 50% of the profile height) of 2.6 keV while exhibiting an asymmetric profile. On the other hand, the ions from the colliding plasmas exhibit a width (at 50% of the profile height) of 1.8 keV (30% narrower than a seed plume) with a quite symmetric distribution. We can also see from figure 2 that the (instantaneous) peak current from the colliding plasma is enhanced approximately three fold compared with that of a single plasma or by $\sim$50% compared with the numerical sum of the left and right seed plumes.

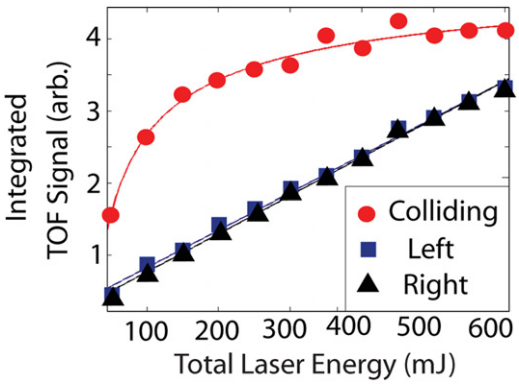

Figure 3. Variation of the time integrated ion TOF signal, normal to the target surface, with incident laser energy for colliding plumes. In the case of the left and right seed plasmas the total energy was split equally between them, so the energy in each focal spot was half the value shown on the horizontal axis.

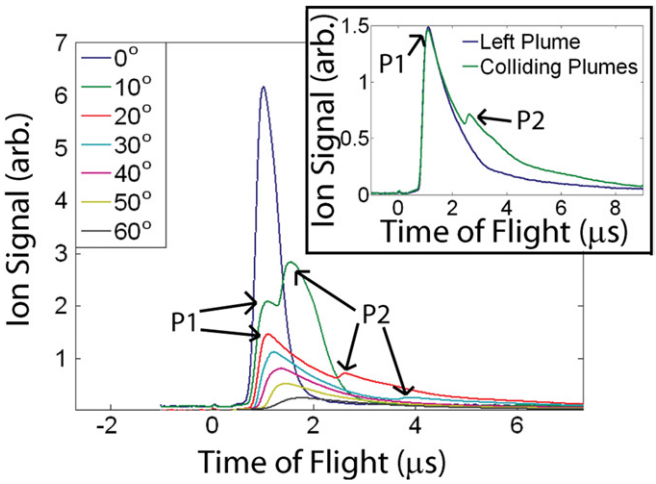

Figure 4. Main: angle-resolved TOF signal for colliding plasmas for a range of angles of detection (main). Inset: comparison of the colliding plasma TOF signal with that of a single plasma plume at a detection angle of 20°.

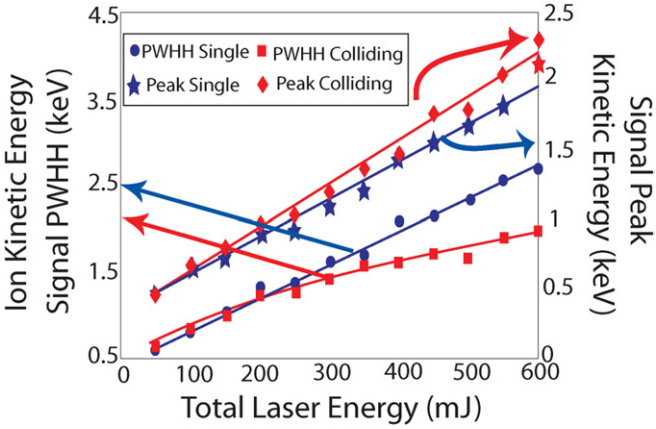

Figure 5. The variation of the profile width at half height (PWHH) and peak position of the ion energy distribution normal to the target with incident laser energy for colliding plumes. The arrows point to the relevant axes for each trace. In the case of the single plasma plume the total energy into the focal spot on the target was 100% of the value shown on the horizontal axis. In the colliding plasma case the total energy in each of the seed plasmas was 50% of the values shown.

Figure 3 shows the dependence of the integrated TOF signal, normal to the target surface, as a function of incident laser energy. The data points were obtained by integrating the traces in figure 2 for total laser energies in the range 100–600 mJ. A departure from linearity is observed in the case of the colliding plasma system compared with the single seed plumes. It is evident from figures 2 and 3 that the ion emission, normal to the target, from the colliding plasmas is clearly not a simple numerical sum of those from the seed plumes. Although the full explanation for our observations will require detailed modelling we suggest a couple of processes which will need to be taken into account. In the early stages of stagnation layer formation (first few tens of nanoseconds) we know that electron stagnation occurs [21] and so the prompt highly charged ions from the seed plumes are likely to experience a local accelerative force. Hence we would expect to see an increase in the number of ions at higher kinetic energies close to the peak or cut-off energy. However, as time progresses, ion stagnation is established, and the stagnation layer can build up a net positive sheath which can result in Coulomb blocking of the slow ions from each seed plasma. Additionally, as time proceeds, slow ions can be lost in collisions with the stagnation layer. We suggest that all of these processes (and perhaps others) can act in consort to reduce the low energy ion flux.

Figure 4 (main) shows the angle-resolved ion TOF signal from the colliding plumes. A narrower energy distribution is observed only in the direction normal to the target and the angle-resolved integrated flux can be fitted by a $\cos^n$ function [29] similar to the single plasma plume case [30]. It is also evident from figure 4 that the ion signal, in the colliding plasma case, splits into two distinct peaks, labelled P1 and P2, when the Faraday cup is moved to angles between 5° and 30° either side of the target normal. The first peak, P1, is due to ions emerging from a seed plasma plume and arriving at the detector which appear to be largely unaffected by the presence of the stagnation layer. This is clear from figure 4 (inset) where it can be seen that the first peak, P1, of the colliding plasma signal matches extremely well with the ion TOF signal from the left seed plasma plume only. The amplitude and kinetic energy of P2 decrease rapidly as the detector is rotated away from the target normal. Beyond ±20° P2 is severely diminished and has disappeared completely for angles greater than ±30° where the traces are indistinguishable from the single plasma plume case. Therefore, we conclude that P2 is due predominantly to ion emission sensitive to the presence of the stagnation layer which, as can be readily observed in figure 4, is highly directional. This observation stands in stark contrast to emission from single plasma plumes where ions are emitted over a wide range of angles.

Figure 5 reveals the dependence of the peak, i.e. the most probable kinetic energy and the distribution width of the ions emitted from single and colliding plasmas as functions of the incident laser pulse energy, E_L. It is clear from figure 5 that by varying E_L it is possible to tune the kinetic energy distribution of the ions emitted from colliding LPPs. The peak position of the ion energy distribution from colliding plasmas (blue

diamond) increases linearly with E_L. However, the profile width at half height (PWHH) of the distribution for colliding plasmas is proportional to $E_L^{1/2}$. Hence relatively narrow profiles (referenced to the peak position) can be obtained with increasing laser energy. In contrast, in the case of a single plasma, we observe that both the peak position and the PWHH of the ion energy distribution increase linearly with E_L for these plasma regimes.

4. Conclusions

In conclusion, we have measured the angularly resolved ion emission from a laser-produced colliding plasma system. The ions emitted from the stagnation layer, formed in the vicinity of the collision front between two colliding plasmas, were found to possess a narrower and more symmetric kinetic energy distribution than for the single laser plasma case. Both the peak energy and profile width could be adjusted by varying the incident laser energy. The linear dependence of the peak position, and the square root dependence of the profile width, implies a sharper distribution with increasing laser energy. In the future we will extend these studies to include charged resolved measurements, with a compact retarding field analyser currently under development at our laboratory.

Acknowledgments

This work was sponsored by Science Foundation Ireland under grant numbers Science Foundation Ireland (SFI) RFP PHY041 and SFI PI 07/IN.1/I1771 and the Higher Education Authority (HEA) PRTLI IV INSPIRE program of the 2nd National Development Plan (NDP2). PHo and TJK thank the Irish Research Council for Science Engineering and Technology and SSH the DCU International Visiting Fellows Program for financial support. Work done in the frame of EU COST action MP0601.

References

[1] Ramsden S A and Davies W E R 1964 *Phys. Rev. Lett.* **13** 227
[2] Pasquini C, Cortez J, Silva L M C and Gonzaga F B 2007 *J. Braz. Chem. Soc.* **18** 463–512
[3] O'Haire R, McGlynn E, Henry M O and Mosnier J P 2007 *Superlatt. Microstruct.* **42** 468
[4] Tao Y, Tillack M S, Sequoia K L, Burdt R A, Yuspeh S and Najmabadi F 2008 *Appl. Phys. Lett.* **92** 251501
[5] Bulanov S V, Esirkepov T Z, Kamenets F F, Kato Y, Kuznetsov A V, Nishihara K, Pegoraro F, Tajima T and Khoroshkov V S 2002 *Plasma Phys. Rep.* **28** 975
[6] Ganeev R A, Suzuki M, Baba M and Kuroda H 2009 *Appl. Phys. Lett* **94** 051101
[7] Nicolaï Ph, Tikhonchuk V T, Kasperczuk A, Pisarczyk T, Borodziuk S, Rohlena K and Ullschmied J 2006 *Phys. Plasmas* **13** 062701
[8] Kasperczuk A, Pisarczyk T, Kalal M, Ullschmied J, Krousky E, Masek K, Pfeifer M, Rohlena K, Skala J and Pisarczyk P 2009 *Appl. Phys. Lett.* **94** 081501
[9] Kasperczuk A *et al* 2009 *Laser Part. Beams* **27** 115–22
[10] Rambo P W and Denavit J 1994 *Phys. Plasmas* **1** 4050–60
[11] Chenais-Popovics C *et al* 1997 *Phys. Plasmas* **4** 190–208
[12] Goldston R J and Rutherford P H 1995 *Introduction to Plasma Physics* (London: Taylor & Francis)
[13] Rumsby P T, Paul J W M and Masoud M M 1974 *Plasma Phys.* **16** 969–75
[14] Wan A S, Barbee T W, Jr, Cauble R, Celliers P, Da Silva L B, Moreno J C, Rambo P W, Stone G F, Trebes J E and Weber F 1997 *Phys. Rev.* E **55** 6293
[15] Bosch R A, Berger R L, Failor B H, Delamater N D, Charatis G and Kauffman R L 1992 *Phys. Fluids* B **4** 979–88
[16] Remington B A, Haan S W, Glendinning S G, Kilkenny J D, Munro D H and Wallace R J 1992 *Phys. Fluids* B **4** 967–78
[17] Gregory C D, Howe J, Loupias B, Myers S, Notley M M, Sakawa Y, Oya A, Kodama R, Koenig M and Woolsey N C 2008 *Astrophys. J.* **676** 420–6
[18] Smith R A, Lazarus J, Hohenberger M, Marocchino A, Robinson J A, Chittenden J P, Moore A S , Gumbrell E T and Dunne M 2007 *Plasma Phys. Control. Fusion* **49** B117–24
[19] Irissou E, Vidal F, Johnston T, Chaker M, Guay D and Ryabinin A N 2006 *J. Appl. Phys.* **99** 034904
[20] H Luna, K D Kavanagh and J T Costello 2007 *J. Appl. Phys.* **101** 033302
[21] Hough P, McLoughlin C, Kelly T J, Hayden P, Harilal S S, Mosnier J P and Costello J T 2009 *J. Phys. D: Appl. Phys.* **42** 055211
[22] Hough P, McLoughlin C, Harilal S S, Mosnier J P and Costello J T 2010 *J. Appl. Phys.* **107** 024904
[23] Dardis J and Costello J T 2010 *Spectrochim. Acta* B **65** 627–35
[24] Denker A, Homeyer H, Kluge H and Opitz-Coutureau J 2005 *Nucl. Instrum. Methods* B **240** 61–8
[25] Torrisi L, Gammino S, Andò L and Làska L 2002 *J. Appl. Phys.* **91** 4685–92
[26] Woryna E *et al* 2000 *Rev. Sci. Instrum.* **71** 949–51
[27] Yogo A *et al* 2009 *Appl. Phys. Lett.* **94** 181502
[28] Kools J C S, Baller T S, De Zwart S T and Dieleman J 1992 *J. Appl. Phys.* **71** 4547–56
[29] Hough P 2010 *PhD Thesis* Dublin City University
[30] Morris O, Hayden P, O'Reilly F, Murphy N, Dunne P and Bakshi V 2007 *Appl. Phys. Lett.* **91** 081506